Journal of Engineering and Applied Science

RESEARCH Open Access

An effective investigation of chatter prediction system on Al6061 alloy in an end milling process

Trivikrama Raju C[1], Jakeer Hussain S[2*], Yedukondalu G[1] and Murahari Kolli[3]

*Correspondence:
jakeershaik786@gmail.com

[1] Department of Mechanical Engineering, Koneru Lakshmaiah Education Foundation, Vaddeswaram, Guntur, India
[2] Department of Mechanical Engineering, Mother Teresa Institute of Science and Technology, Sathupally, India
[3] Mechanical Engineering Department, Lakireddy Balireddy College of Engineering, Mylavaram, Andhra Pradesh, India

Abstract

Visual examination of the surface topography, in conjunction with the other sensors, may confirm the existence of chatter. Online chatter detection during real machining operations is possible with the use of sensors, and the presence of noise in their output and restricted bandwidth are the major drawbacks of these sensors. Productivity drops and manufacturing costs go up when there is a lot of chatter in the machining process. In the present paper, an integrated spindle tool system is modeled using finite element method with Timoshenko beam theory including rotational and shear deformation effects. To maximize the average stable depth of cut in an end milling process while simultaneously minimizing the chatter vibration levels, real time and offline strategies have been investigated. Machining experiments performed on Al6061-alloy specimens provide an empirical confirmation of the stability boundaries. The surface topography methods such as scanning electron microscope (SEM) and optical microscope images along with vibration levels are considered, to identify chatter marks under various machining conditions, which helps to assure cutting process stability. Stability lobe diagrams are plotted with these derived conditions and observed at an incremental level in the axial depths of the cut. The methodology shown in this paper improves the machining stability of the end milling with the reduction in the tool tip vibrations.

Keywords: Timoshenko beam theory, Chatter, Scanning electron microscope (SEM), Stability lobe diagrams, Al6061-alloy, Optical microscope images

Introduction

Chatter, a self-excited vibration phenomenon, is a major obstacle in machining that negatively impacts stability and surface quality. Chatter not only hampers the pace at which material is removed but also speeds up the deterioration of the tool and undermines the precision of the dimensions, presenting a substantial barrier to attaining the best possible machining performance. Chatter prediction and mitigation are crucial when milling aluminum alloy Al6061, which is often used in aerospace applications because of its favorable strength-to-weight ratio and outstanding machinability. Al6061 has distinct difficulties in machining, such as its inclination to produce built-up edge (BUE) and the creation of elongated, fibrous chips, both of which may worsen vibration tendencies. To

tackle these problems, it is necessary to have a thorough grasp of the intricacies of the end milling process. This includes details of working with tool geometry, cutting parameters, material qualities, and machining conditions which all interact with each other. Experimental validation is crucial for establishing reliable chatter prediction systems that may be efficiently used in industrial settings, notwithstanding the useful insights provided by theoretical models and simulation approaches. Hence, this study seeks to examine the chatter prediction system in the process of end milling Al6061 alloy using an experimental methodology. Through the deliberate manipulation of machining parameters such as cutting speed, feed rate, and depth of cut, and the use of modern sensing and monitoring technology, our objective is to uncover the key characteristics that trigger chatter and create predictive models that can anticipate its beginning.

The frequency responses and stability lobe diagrams of the tool tip are obtained using finite element modeling. The model8s output is used to generate the function values, resulting in the attainment of the highest possible depth of cut that can be sustained without instability. The improved spindle design, which includes a semi-active and active damper at the appropriate location, is important to enhance the cutting stability. The quality of the machined surfaces is negatively affected by vibrations that occur during the machining process. Vibrations like this may lead to issues including machine wear and tear, broken tools, noisy operations, overworked cutting edges, broken machine tools, and worn-out machine tool parts. Previous literature has only given a limited number of the effects of the vibration damper on the integrated spindle tool unit. Analysis of the spindle tool and related flexible body dynamics will help to identify the best machining settings for end milling.

Despite much analytical and experimental effort on spindle models, very few research has been published in reducing the chatter using the surface texture methods. Models were presented by Altintas and Budak [1]; they used the tool point frequency response function (FRF) to forecast stability areas. When trying to model the spindle, tool holder, and bearing system to forecast their dynamic behavior, Chao et al. [2] took the joint properties into account. Additionally, these models have been validated by experiments. While investigating the significance of the electronic position and speed of the spindle in achieving precision in the SLD, Raphael and Reginaldo [3] enhanced the accuracy of stability lobes. Using finite element modeling, Hung et al. [4] demonstrated how the machining stability is affected by the contact between the spindle and machine frame.

Albrecht et al. [5] analyzed the two-dimensional cutting force model along with the evaluation of the displacements for spindle tool system. A displacement sensor is mounted on the spindle portion to measure the dynamic fluctuations observed between the head of the sensor and revolving unit of the spindle during the machining. Park and Altintas [6] developed a new integrated force sensor system for the spindle tool unit, which incorporates dynamic compensation to accurately measure cutting forces. Stationary spindle housing was equipped with integrated piezo-electric force sensors. As part of this dynamic structural model, a relationship model was established between the cutting forces produced at the tool tip and the forces produced at the spindle housing. Jang and Tarang [7] utilized a novel piezoelectric actuator to measure the active vibrations developed during the machining of the workpieces. By adjusting the inertial mass, the resonance of the actuator may be fine-tuned across a wide frequency range. Because

of this, the actuator can reduce undesirable vibrations by applying a strong damping force. In their development of the flexible model of the constructed spindle tool unit, Duncan et al. [8] used receptance coupling approaches. This enhanced model includes the dynamic absorber effect, which resulted in improved dynamic stiffness which in turn leads to the stability of the machining process. Madoliat et al. [9] suggested with a frictional damper to enhance the damping of the structure and prevent the self-excited vibrations in the case of thin-walled end milling. Several parametric studies were undertaken to determine the optimal settings of the damper to enhance the stability limit. An active control mechanism was devised by Parus et al. [10] to reduce chatter vibration. To successfully lessen the cutting vibrations, the active control system that was proposed used a piezoelectric actuator in conjunction with the quadratic Gaussian algorithm. Madoliat et al. [11] provided a comprehensive study on the slender end milling tools with the application of a frictional damper. A precise numerical model was constructed for this damper, which accurately incorporates friction modeling in both sliding and pre-sliding areas. Regib et al. [12] introduced a technique for controlling spindle speed to reduce machine tool noise. The approach included adjusting the spindle speed to minimize the energy required by the cutting operation.

In their study, Sulaiman et al. [13] proposed a method for mitigating chatter during the machining of Ti-6Al-4 V in an end milling process. The chatter mitigation had been done by using the ferrite magnets and the vibrations are minimized. A separate customized attachment was created and installed on the spindle of the end milling machine tool center to secure the permanent magnet bars, which are used to reduce the amplitudes of vibration.

Monnin et al. [14, 15] introduced a dynamic system that is included into a spindle unit and utilizes two distinct optimum control algorithms. To lessen the effect of cutting forces on tool tip deviations, the initial method was integrating machine structural dynamics into controller design. Graham et al. [16] developed different methods such as zero-exclusion condition and edge theorem to produce the robust analytical chatter model for the end milling. The dependability was enhanced in comparison to the predicted pseudo-one degree of freedom model. Moradi et al. [17] developed a new tunable vibration absorber with the purpose of mitigating regenerative chatter during the milling process of cantilever plates. The absorber location and spring stiffness were optimized to minimize plate vibration during regenerative chatter situations. Zhang et al. [18] devised an active control model for the machining workpieces in end milling process, which significantly expanded region of cutting stability without noise along with improved efficiency of the process.

Using the time series cutting force model, Rafal et al. [19] investigated the milling stability of the titanium alloy (Ti6242). To find the initial value of the chatter vibrations, the Hilbert-Huang transform (HHT) and the recurrence quantification analysis were used. Thread milling, weld cutting, and drilling are just a few of the machine activities that Wu et al. [20] incorporated utilizing robots. To improve the stability of the machining process, many models for reducing vibration are used.

Navid et al. [21] modeled the two-degree freedom model with the consideration of process damping effect as well as tool wear. Vibration absorbers are utilized for the dynamic model to achieve higher metal removal rates. Vineet and Ramesh babu [22] presented

a comparative study of stability lobe diagrams and cutting force coefficients at different spindle speeds with different absorbers. Vinh et al. [23] implemented a post dependent controller using the Gaussian progression method to achieve the maximum stable depth of cuts for the industrial robots with the six degrees of freedom. Jeremie et al. and Rahul et al. [24, 25] proposed active structural methods to mitigate the self-excited vibrations and designed a controller to reduce the cutting forces. When it comes to thin-walled end milling, Madoliat et al. [26] came up with a frictional damper to decrease chatter. Hans Christian and Kim [27] designed a lightweight shell end mill with a semi-active damper system to increase the metal removal rates. Chen and Lu [28] developed tuned vibration absorber for the reduction of the vibrations induced to the end milling process and obtained the optimal process parameters during the milling process. Santiago et al. [29] utilized the perturbation methods and developed a magnetorheological damper device to suppress the vibrations for the milling of thin-walled components. Yang and Yu [30] investigated the surface quality and tool wear for the case of machining the long slender jobs by utilizing the passive dampers and further experiments are carried out to validate the numerical simulations. Lucia et al. [31] investigated the machining characteristics of the Titanium alloy with the optical profilometer and SEM images. Gdula and Mrówka-Nowotnik [32] examined the surface morphology of multi-axis cutting with various operational parameters on the Inconel alloy. The tool wear was analyzed with the kinematics of multi axis cutting as well as with the different profile angles of the cutting tool.

The literature on surface topography is limited, and analysis of the workpiece to determine the correct stability points is, however, severely lacking. Finding the proper stability limits for end milling is the goal of the current work. The analytical stability lobe diagrams were created using the modal data of the spindle tool assembly. The model is tested by cutting tests at various depths of cuts, and these boundaries are validated by the SEM and optical microscope images along with vibration signals at different conditions.

Methods

The objective of this study was to enhance the end milling process by minimizing chatter vibration levels and enhancing stability. This was accomplished by combining finite element approaches, real-time monitoring via sensors, and experimental validation.

The study utilized a blend of numerical modeling and experimental validation. The numerical simulations utilized finite element methods, notably adding Timoshenko beam theory to accurately consider rotational and shear deformation effects in the combined spindle tool systems. Al6061-alloy specimens were experimentally validated in a controlled machining environment. The work utilized Al6061-alloy specimens for experimental validation. The selection of these specimens was based on their frequent utilization in machining applications and their characteristic features, which make them suitable for investigating chatter vibration. The modeling of integrated spindle tool systems was conducted using finite element methods. The Timoshenko beam theory was utilized to precisely depict the rotational and shear deformation effects that occur during machining. Sensors were employed for instantaneous monitoring during milling processes. These sensors offer input on several characteristics, such as vibration levels, enabling real-time modifications to be made to machining parameters.

Experimental validation was performed on Al6061-alloy specimens to confirm the stability bounds obtained from the numerical simulations through machining tests. Multiple milling settings were examined, and surface topography analysis techniques, such as scanning electron microscope (SEM) and optical microscope pictures, were employed to detect and characterize chatter marks. Stability lobe diagrams were constructed using the established criteria resulting from both numerical simulations and experimental verification. Additionally, vibration levels were monitored during these studies to evaluate stability in machining. These diagrams were employed to depict stability boundaries at various axial depths of cut, facilitating comprehension of machining stability and parameter optimization. The study utilized a comprehensive strategy that integrated numerical modeling, real-time monitoring, experimental validation, and visualization approaches to enhance the end milling process and decrease chatter vibration levels.

Finite element modeling of the damper system

Self-excited vibrations, often known as chatter, are the predominant kind of vibration in machining processes. With the process of regeneration mechanism or with the mode coupling phenomenon, there has been a huge occurrence that chatter is possible in the machine tool system. It is possible as there is a difference in phase between the outer waves and inner waves observed in the machining of the workpieces which leads to dynamic gain as well as the instability of the system. The integrated model with spindle assembly, which is presented in Fig. 1, is designed to determine the response of frequency at the tool tip. Components of this integrated model (i.e., tool, holder, and spindle) is discretized with the Timoshenko beam theory, which incorporates rotational and shear deformation, for finite element modeling. The model

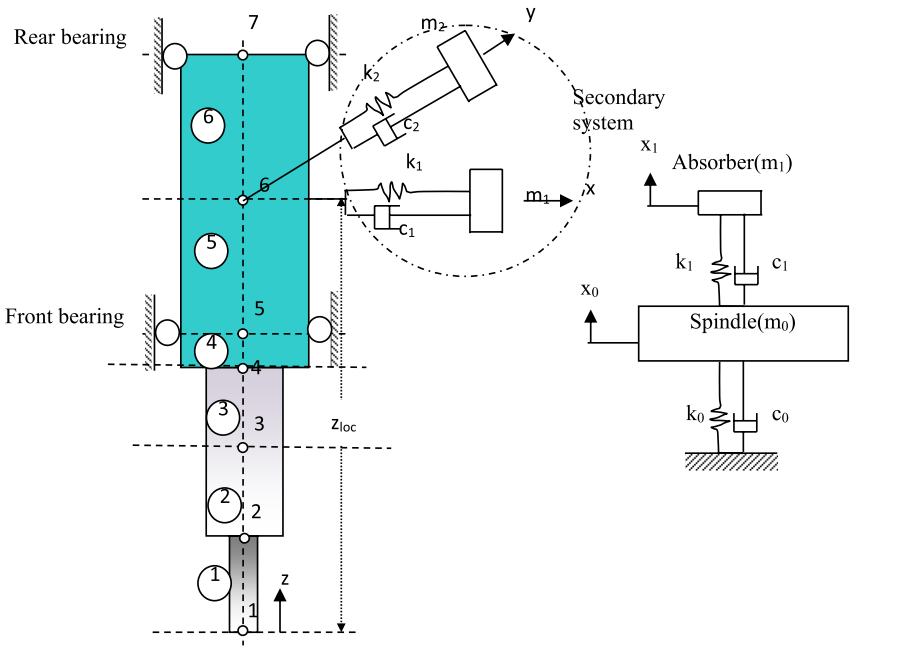

(a) Absorber system in spindle (b) Representation of system in X-direction

Fig. 1 Spindle tool discretization with the absorber system

included detailed geometric representation, material properties, appropriate element discretization, and boundary conditions. Tunable vibration absorbers are often used to minimize chatter in the milling process. The current study presents the cutting tool as a flexible component and the work piece as a stiff portion.

In the present study, it is assumed that cutter is made to account for the potential vibrations and dynamic behaviors during machining. By using the Timoshenko beam formulation, each node with two translational (u_x,v_y) and two rotational degrees of freedom (corresponding slopes θ_x, θ_y) under shear deformation effect is considered for the analysis. The spindle tool unit consists of six distinct elements with seven nodes, each node with four degrees of freedom (DOF), resulting in a total of 28 DOF, and is used to analyze the system with finite element method shown in Fig. 2. This comprehensive modeling approach provided valuable insights into the stability and vibration characteristics, contributing to the optimization of machining processes.

The main spindle mass is considered as m_0, and m_1 and m_2 are the masses of the vibration absorbers with respect to the ground, $P(t)$ is the main force applied to the main mass of the system, and x_0 and y_0 are the displacements of the main spindle system respectively. Similarly, the main mass of the system is linked to the ground with the two bending directions and has the stiffness values as k_1 and k_2 along with the constant viscous damping constants as c_1 and c_2 respectively. In two bending directions, the equations of governing motion are provided as follows:

$$m_0\ddot{x}_0 + c_0\dot{x}_0 + c_1(\dot{x}_0 - \dot{x}_1) + k_0x_0 + k_1(x_0 - x_1) = P(t) \tag{1}$$

$$m_1\ddot{x}_1 + c_1(\dot{x}_1 - \dot{x}_0) + k_1(x_0 - x_1) = 0 \tag{2}$$

$$m_0\ddot{y}_0 + c_0\dot{y}_0 + c_2(\dot{y}_0 - \dot{y}_1) + k_0y_0 + k_2\left(y_0 - y_1\right) = P(t) \tag{3}$$

$$m_2\ddot{y}_1 + c_2(\dot{y}_1 - \dot{y}_0) + k_2\left(y_1 - y_0\right) = 0 \tag{4}$$

The expression for the evaluation of displacements in the frequency domain as follows:

$$x = P \times [H(\omega)] \tag{5}$$

In the above expression, *[H(ω)]* represents the function of frequency response and defined as follows.

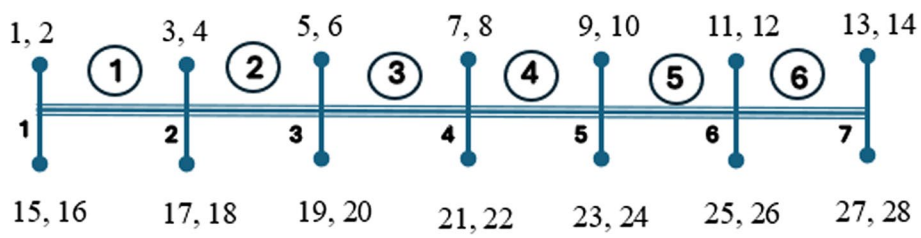

Fig. 2 Element discretization with node numbering

$$[H(\omega)] = \left(-\omega^2[M] + i\omega[C] + [K]\right)^{-1} \tag{6}$$

Specifically, the spindle relates to a spring mass damper system at two different positions in x and y directions respectively. For this spindle tool model, the boundary conditions comprise the forces acting on the bearing nodes in two bending directions as well as the forces exerted by absorber system (i.e., secondary forces) at the linked node. In this design, the fluctuating forces related to cutting are not considered for the analysis. The fifth and seventh nodes of the model are supported by a pair of regular angular contact bearings in both bending directions, as the tool holder of the system must securely grip the tool and be attached to the spindle shaft. These angular bearings projected a diverse behavior of the stiffness and depends on the load and position and on the design of the bearings. Several empirical formulae have been documented in the literature review to analyze the radial stiffness of the axial bearings in the static condition. This stiffness behavior is dependent on factors such as number of balls in the bearing races (N_b), diameter of balls (D_b), and preload of the bearings (F_a) as well as on the contact angle of the bearings (Θ).

$$K_{xx} = K_{yy} = 1.77236 \times 10^7 \times \left(N_b^2 D_b\right)^{1/3} \frac{cos^2\theta}{sin^{1/3}\theta} F_a^{1/3} N/m \tag{7}$$

These stiffnesses were included in the overall governing equations of mass and stiffness matrices and at the bearing nodes of the assembly.

Two-dimensional cutting dynamics

The cutting pressures induce the displacement levels in both X and Y directions which leads to develop the self-excited vibrations in the entire machine tool in both the normal and feed directions. The cutting tool engaged with the workpiece and varied with the time period as $\varphi_j(t) = \Omega t$ with spindle rotates at an angular velocity of Ω (rad/s). The variability of the total chip thickness in the radial direction is determined by the following equation:

$$h(\varphi_j) = \left(f_t sin(\varphi_j) + n_{j-1} - n_j\right) g(\varphi_j) \tag{8}$$

The regulating function g (ϕ_j) has a value of 1 when the jth cutting tooth is employed and 0 otherwise. These analytical cutting forces projected normally and tangentially on to the x and y axis with the cutter rotational angle (ϕ_j) are represented as

$$F_x = \sum_{j=1}^{N_t} k_t b f_t sin(\varphi_j) cos(\varphi_j) + k_n b f_t sin(\varphi_j) sin(\varphi_j) \tag{9}$$

$$F_y = \sum_{j=1}^{N_t} k_t b f_t sin(\varphi_j) sin(\varphi_j) - k_n b f_t sin(\varphi_j) cos(\varphi_j) \tag{10}$$

Here, feed per tooth is represented as f_t, axial depth of cut a b, and k_t and k_n are the cutting force coefficients due to shearing action in the tangential and radial direction.

To obtain the analytical stability lobe diagrams for an end milling in two dimensions, the following characteristic equation is used as follows:

$$det([I] + +\Lambda[FRF_{or}]) = 0 \tag{11}$$

where the FRF_{or} is the oriented frequency response, and variable "Λ" is mathematically represented as

$$\Lambda = -\frac{N_t}{4\pi} bK_t \left(1 - e^{-i\omega_c \tau}\right) \tag{12}$$

$$[FRF_{or}] = \begin{bmatrix} \alpha_{xx}FRF_{xx}(i\omega_c) + \alpha_{xy}FRF_{yx}(i\omega_c) & \alpha_{xx}FRF_{xy}(i\omega_c) + \alpha_{xy}FRF_{yy}(i\omega_c) \\ \alpha_{yx}FRF_{xx}(i\omega_c) + \alpha_{yy}FRF_{yx}(i\omega_c) & \alpha_{yx}FRF_{xy}(i\omega_c) + \alpha_{yy}FRF_{yy}(i\omega_c) \end{bmatrix} \tag{13}$$

The terms α_{xx}, α_{xy}, α_{yx}, and α_{yy} are the directional orientation factors and rely on the selection of the entry φ_s and exit φ_e angles of the cut.

The frequency dependent characteristic equation with the eigen values is written as follows:

$$\begin{gathered} a_0\Lambda^2 + a_1\Lambda + 1 = 0 \text{ where} \\ a_0 = \left(\alpha_{xx}FRF_{xx}(i\omega_c) + \alpha_{xy}FRF_{yx}(i\omega_c)\right) \times \left(\alpha_{yy}FRF_{yy}(i\omega_c) + \alpha_{yx}FRF_{xy}(i\omega_c)\right) \\ -\left(\alpha_{xx}FRF_{xy}(i\omega_c) + \alpha_{xy}FRF_{yy}(i\omega_c)\right) \times \left(\alpha_{yx}FRF_{xx}(i\omega_c) + \alpha_{yy}FRF_{yx}(i\omega_c)\right) \\ \text{and} \\ a_1 = \alpha_{xx}FRF_{xx}(i\omega_c) + \alpha_{xy}FRF_{yx}(i\omega_c) + \alpha_{yx}FRF_{xy}(i\omega_c) + \alpha_{yy}FRF_{yy}(i\omega_c) \end{gathered} \tag{14}$$

From the above equation, the complex eigen values Λ_1 and Λ_2 can be determined by the quadratic equation.

The corresponding limiting depth of cut at the spindle speed can be obtained from these equations as follows.

$$b\frac{2\pi Re(\Lambda)}{NK_t}\left(1 + \left(\frac{Im(\Lambda)}{Re(\Lambda)}\right)^2\right)_{lim} \tag{15}$$

$$\Omega = \frac{2\pi\omega_c}{N_t}\frac{60}{(\lambda + 2\pi N)} \tag{16}$$

$$\lambda = \pi - 2tan^{-1}\left(\frac{Im(\Lambda)}{Re(\Lambda)}\right) \tag{17}$$

The stability lobe diagrams are plotted from b_{lim}, and Ω and N represents the individual lobe number starting from the left to right.

Geometrical dimensions of the spindle tool unit

Table 1 depicts the geometrical and material details that have been used in the modeling of integrated spindle tool unit.

A numerical program was built in MATLAB environment, as to examine dynamics of the coupled spindle tool system in addition with the vibration absorber system. By using Rayleigh damping method, the coefficients of $\alpha = 17.32$ and $\beta = 3.65\text{e}-6$ are determined with a damping ratio of 1% and the same is considered for the analysis. The characteristics of the stiffness value for the angular contact bearings primarily depends on the

Table 1 Details of material and geometric properties

Dimensions of the model	E1	E2	E3	E4	E5	E6	E7
Length (mm)	30	85	85	51	60	45	45
Outer Dia (mm)	12	40	40	75	75	75	75
Inner Dia (mm)	0	0	0	40	0	0	0
Youngs Mod (E) Pa	2.8e11	2.1e11	2.1e11	2.1e11	2.1e11	2.1e11	2.1e11
Density (Kg/m^3)	7972	7850	7850	7850	7850	7850	7850

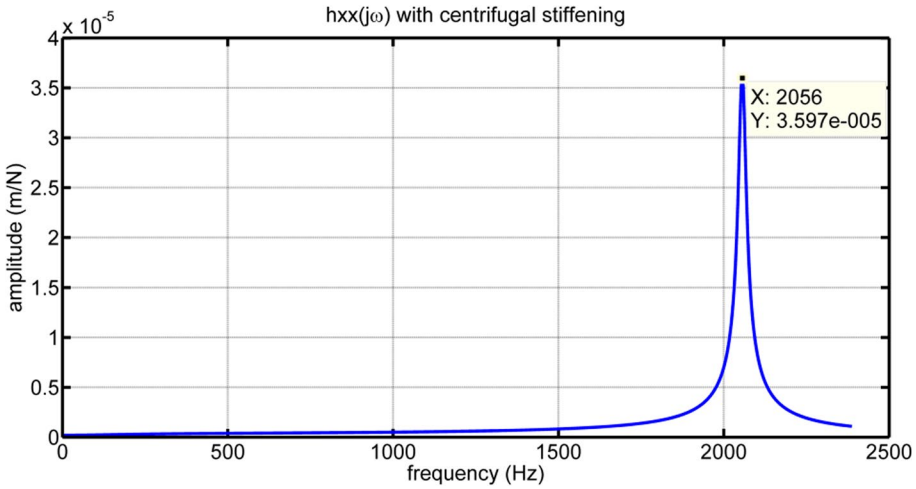

Fig. 3 Absolute tool tip frequency response

position on the spindle along with the applied bearing preload. The spindle system is modeled using the following bearing parameters: the ball's diameter (D_b) is 9 mm, and an axial preload of 1500 N (F_a) is applied. The angular contact of the ball-bearing (θ) is 25°, and there are 20 balls (N_b) in total. At the tip of the tool, frequency response is evaluated by considering the vibration absorber parameters as the damper mass ($m_1 = m_2$) is 1 kg, the stiffness for the absorber as ($k_1 = k_2$) is 1.5e5 N/m, and the absorber damper value ($c_1 = c_2$) is 1.5 N-s/m. It is evident from Fig. 3 that the first predominant modal frequency value is 2056 Hz.

In order to evaluate this response (h_x ($j\omega$)) tool tip, the dynamics of bearing along with the centrifugal stiffening effect is included in the program, and this is carried out at a specific spindle speed of 3000 rpm (Ω). In addition to this, convergence tests carried out for the model to determine adequacy of the model. This test would also check that the solution stabilizes and approaches a consistent result as the mesh becomes finer, and it also ensures that the numerical solution is not heavily dependent on the mesh size. Table 2 shows that the frequency value remains constant after the seventh element.

Experimental results

Furthermore, an experiment sine sweep testing is carried out on a CNC three-axis machining center (MTAB-Maxmill) to validate the numerical analysis. An experimental modal analysis is conducted for the spindle tool holder system of CNC milling

Table 2 Convergence test results to reduce the discretization errors

No. of elements	Frequency values in Hz from FEM
3	2034.8
5	2047.6
7	2056.4
8	2056.4
10	2056.5

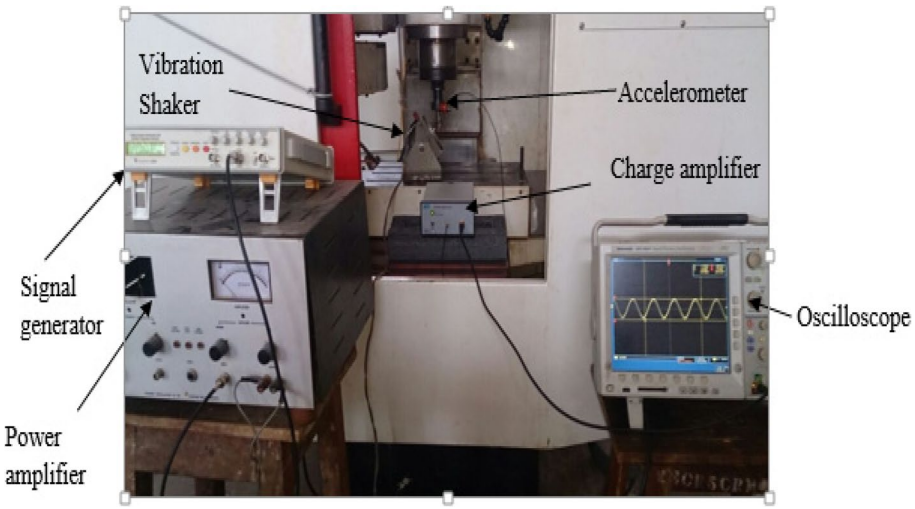

Fig. 4 Experimental sine sweep testing

center (make: MTAB-Maxmill) available at NIT central workshop. The three-axis machine tool has a single-phase AC synchronous motor driving the spindle at variable speeds. A four-fluted HSS end mill cutter with 12-mm diameter and a tool holder BT40 ER32 COLLET CHUCK MAS 403 (DIN 6499) is utilized to hold the end mill cutter. In order to obtain the modal information of spindle tool unit, the following instrumentation is employed: (i) 4-channel digital oscilloscope (model-DPO 43034 for recording time histories), (ii) a power amplifier (model SI-28), (iii) an accelerometer (PG 109 M0, frequency range 1 to 10,000 Hz), (iv) a charge amplifier (model: CA 201 A0, maximum output voltage $\pm$ 5 V, frequency range 0.2 Hz to 15 kHz), (v) a signal generator, and (vi) vibration shaker (type: V-6–27,050). The time histories are measured with a four-channel digital oscilloscope, to amplify the input power signals with a power amplifier; an accelerometer sensor is used to detect the vibration levels in the integrated spindle model, a signal generator is utilized to produce the waveforms varies with frequency of input over time, and a vibration shaker is utilized to generate the sinusoidal vibrations with varying frequencies. Figure 4 depicts the arrangement of these measuring devices on the CNC milling machine to evaluate the responses at the tool tip.

A power amplifier is utilized to systematically change the signal's frequency while keeping its amplitude constant. An oscilloscope records the accelerometer readings

at each frequency level when the spindle tool is stimulated by the vibration shaker. Furthermore, these signals were analyzed and plot the frequency-dependent amplitudes of the system's time-domain response for each functional frequency as shown in Fig. 5.

The identified resonant frequencies hold significant implications for the spindle tool system under investigation. It is observed that there is an agreement between the experimental observations, and the numerical model strengthens the validity of the results. The resonance peaks at 2039 Hz and 2590 Hz denote critical frequencies and are in close agreement with the numerical results.

Results and discussions

By utilizing the numerically arrived frequency response date, the analytical stability lobe plots are created by utilizing the following properties, which includes modal properties as follows: stiffness values in X and Y direction $k_{xx}=k_{yy}=2.1\text{e}8$ N/m, natural frequencies $\omega_x=\omega_y=2056$ Hz, and damping ratio values as $\xi_x=\xi_y=0.01$. The supplementary requirements consist of a tool diameter of 12 mm, an average specific cutting pressure of 750 N/mm^2 (specific to aluminum alloy 6061), and a fixed number of teeth (N_t) of 4. The stable and unstable zones in the slot milling operation are obtained by utilizing tool tip frequency response data which arrived from the finite element analysis. Few data points are selected for the identification of unusual chatter vibrations at different axial depths, and spindle speeds were measured using a setup that includes a four-channel digital oscilloscope, an accelerometer, and a charge amplifier positioned at the workpiece as displayed in Fig. 6.

The vibration signals of the cutting tool are captured in the time domain using a four-channel digital oscilloscope. Peaks in the frequency spectrum corresponding to the chatter frequencies observed in vibration data confirmed the presence of chatter. In contrast, a smooth frequency spectrum without significant peaks indicated stability. Figure 7 displays a set of graphs depicting the time histories and fast Fourier

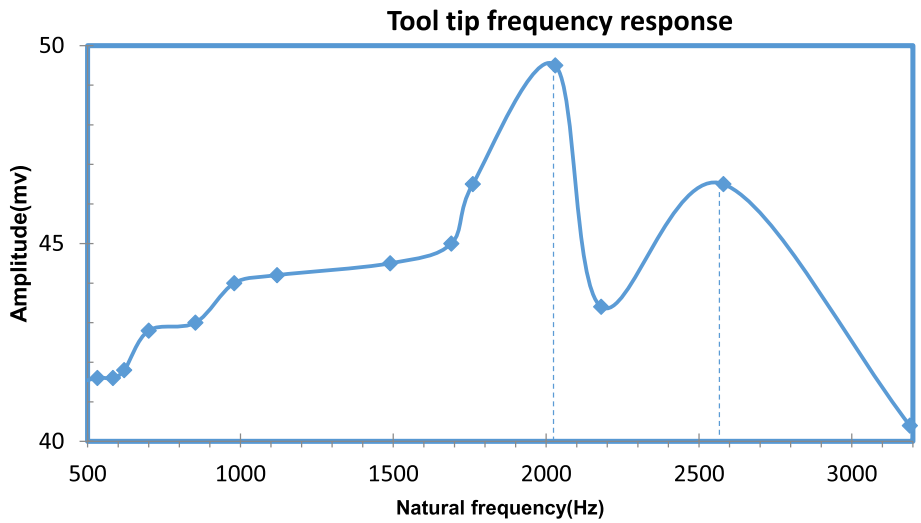

Fig. 5 Frequency response of the spindle tool unit using sine sweep testing

Fig. 6 Experimental setup utilized for machining

transform (FFT) plots corresponding to different depths of cut. These plots unveil a clear pattern: as the axial depth of cut increases, there is a concurrent rise in the amplitude of vibration levels during machining, leading to the formation of chatter marks on the workpiece. The onset of chatter is anticipated to occur early in the cutting process as the depth of cut escalates.

Surface topography refers to the detailed surface texture and finish of a machined part and significantly influenced by the presence of chatter during machining operations. Surface texture, including the periodicity and pattern of tool marks, was analyzed. Optical microscopy and scanning electron microscopy (SEM) were used to visualize the surface patterns. Regular, evenly spaced tool marks indicated stable cutting, while irregular, overlapping, or erratic patterns were indicative of chatter.

Scanning electron microscopy (SEM) images of aluminum alloy Al6061 may provide vital information on its microstructure, surface properties, and any faults that may affect machining procedures such as end milling. However, predicting the chatter in an end milling machine based on SEM images is quite complex. The images shown in Fig. 8 reveal the features like grain structure and potential defects that occurred during the machining process such as voids, inclusions, or cracks. These factors are essential to estimate the chatter deeply and identify any anomalies that might affect the machining. It is observed that in Fig. 8a, b, less voids are identified, whereas in Fig. 8c, d, more voids and inclusions are formed as the depth of cut increased.

The machined surface was examined using an optical microscope with a magnification factor of $\times 10$. As depicted in Fig. 9, the optical microscope images illustrate the presence of chatter marks on the workpiece material at different axial depths of cut across various spindle speeds measured in rotations per minute (rpm). These images distinctly indicate the occurrence of indentation marks on the work surface when the machining zone traverses into regions prone to chatter, particularly noticeable when the cutting depth exceeds 0.19 mm.

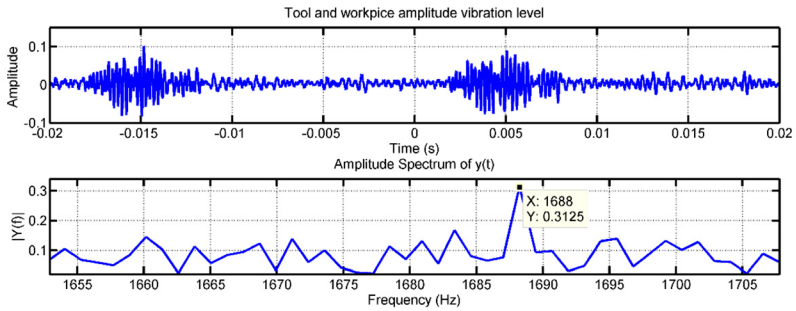

(a) Vibration level at a depth of 0.11mm

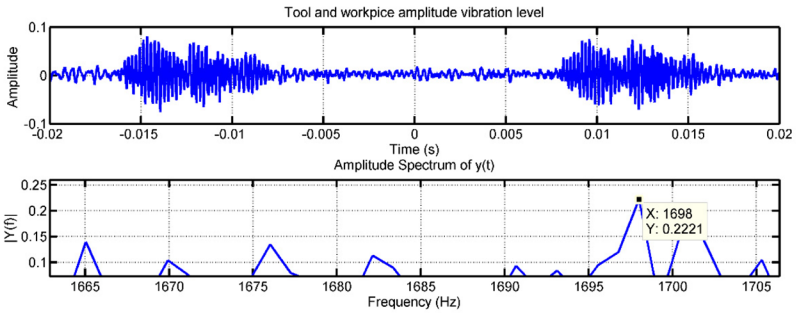

(b)Vibration level at a depth of 0.14mm

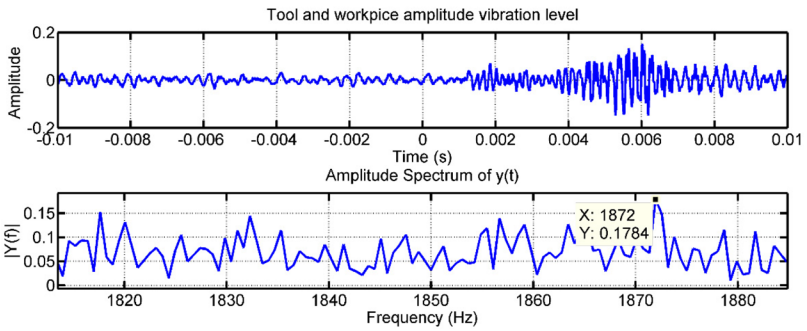

(c)Vibration level at a depth of 0.19mm

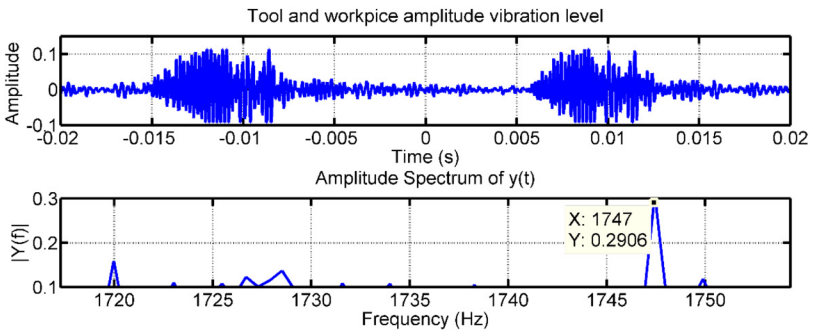

(d) Vibration level at a depth of 0.28mm

Fig. 7 FFT plots at different axial depths of cut

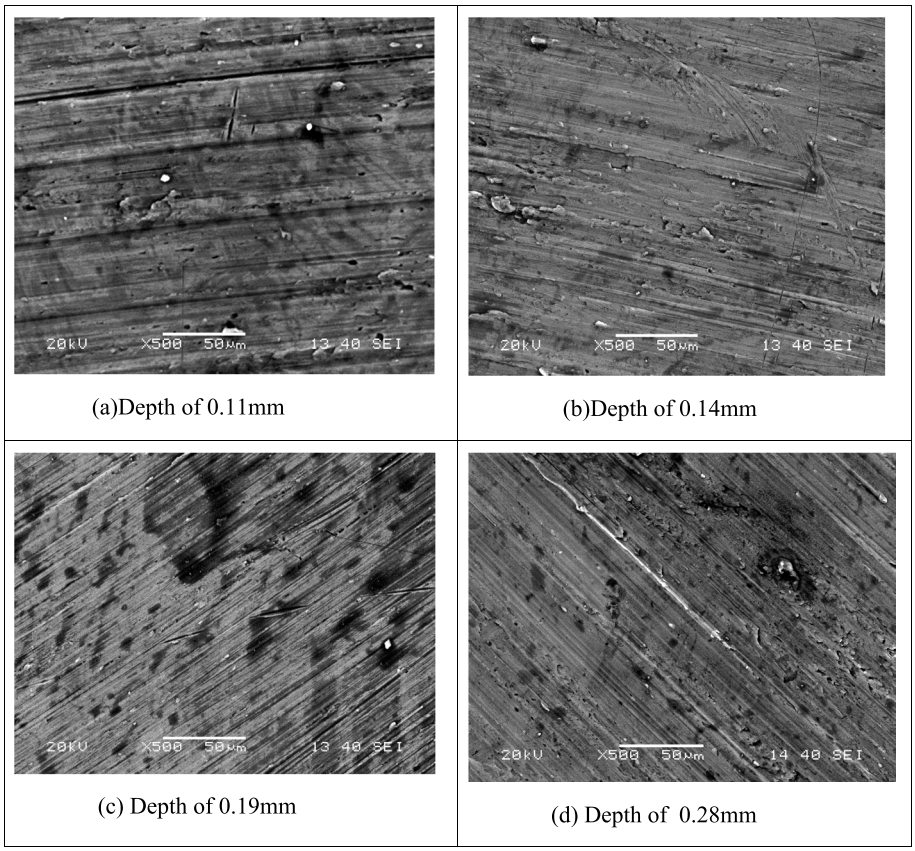

Fig. 8 SEM images of the machined surface at different depths of cut

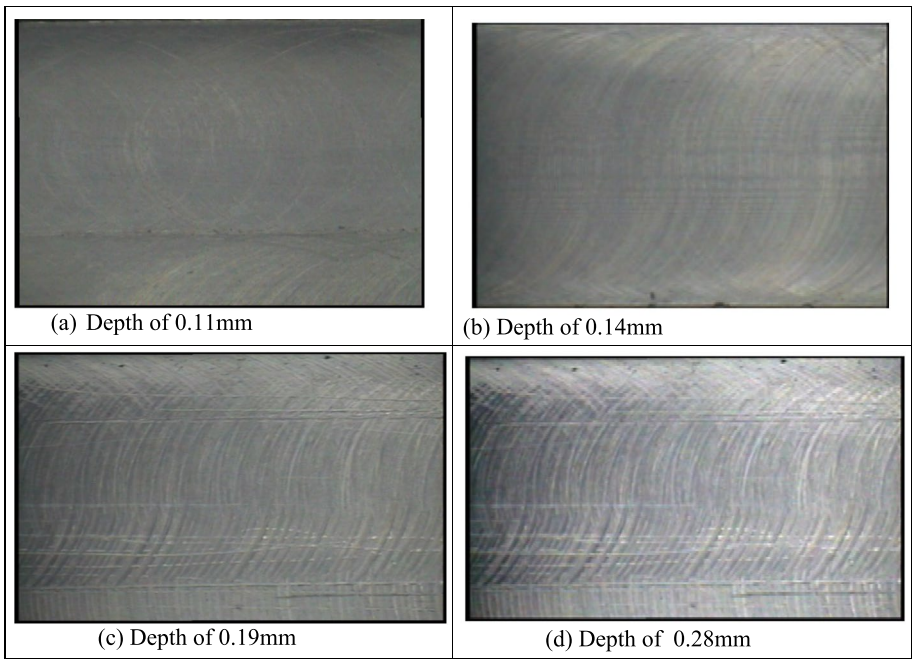

Fig. 9 Optical surface images of the machined surfaces at the different depths of cut

The accuracy of these analytical stability lobe diagram (SLD) is confirmed by interpolating data points obtained from vibration levels measured during tool machining and optical microscope surface images at the appropriate machining conditions. Based on this data, the circular markers (**o**) represent the stable cutting points, whereas the square markers (□) indicate unstable cutting results in chatter marks on the workpiece. Theoretical lobe, as depicted in Fig. 10, demonstrates a close correspondence with the boundaries of the experimental data points.

Conclusions

In the present paper, a passive method of vibration absorption system is developed, and the corresponding stability studies were investigated. The integrated spindle tool model was analyzed with Timoshenko beam theory by considering the effects of rotating inertia and shear deformation of the spindle shaft. Tool tip frequency response arrived numerically and further compared with the experimental sine sweep testing method and observed a considerable agreement between the results. A damper system is developed and observed the reduction in the vibration amplitude. The passive system demonstrated a significant reduction in tool tip vibration amplitudes by approximately 20–30% across various cutting conditions. There was a substantial agreement between the numerical and experimental FRFs, validating the accuracy of the simulation models in predicting the reduction in vibration amplitudes.

Analytical lobe diagrams arrived at the machining conditions, and further experimental cutting tests were conducted to investigate the stable boundaries with the use of vibration signals; SEM and optical microscope images were utilized. By integrating SEM analysis with other factors relevant to machining dynamics, they were able to develop a more comprehensive understanding of chatter in end milling processes and improve prediction accuracy. It is observed that, during the machining of Al6061 with these conditions, a smaller depth of cut with lower feed and higher spindle speed is effective in reducing the vibration levels thereby produced the quality machining surface. This analysis demonstrated the productivity gains with improved stability, increasing depth of cut and feed rates by 35–40%, with the optimized machining conditions, highlighting the effectiveness of the proposed approach. The incidence of

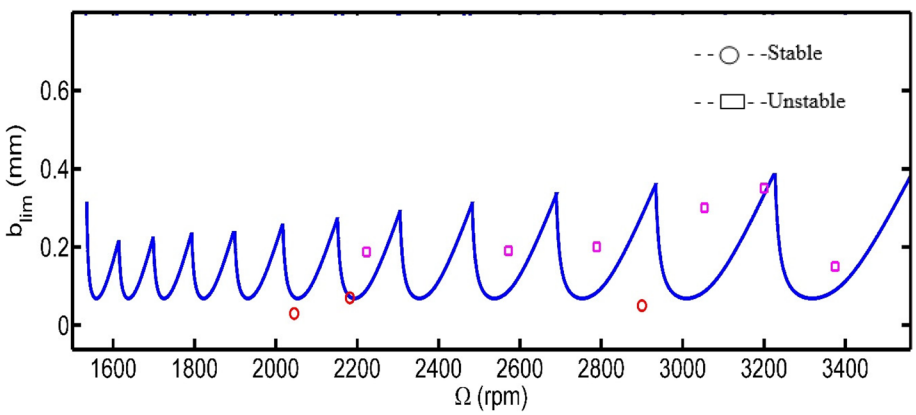

Fig. 10 Experimental verification of analytical lobe diagram

chatter marks on the machined surface was notably reduced, resulting in higher quality finishes. Higher feed rates were achievable with the vibration absorption systems, improving overall machining efficiency and productivity.

The use of numerical simulations and practical cutting tests provides significant and necessary knowledge about the dynamic characteristics of spindle systems under different spindle process settings and offers practical implications for enhancing the performance of spindle systems in diverse machining conditions. These results in the paper highlight the crucial need of sophisticated chatter identification methods in dealing with the dynamic problems in end milling operations.

Abbreviations

SLD	Stability lobe diagrams
SEM	Scanning electron microscope
FFT	Fast Fourier transform
$K_{xx} = K_{yy}$	Static radial stiffness of the bearing
N_t	Number of teeth of the cutter
b_{lim}	Average stable depth of cut obtained from the lobe diagram
$m_1 = m_2$	Mass of the damper
$k_1 = k_2$	Stiffness of the absorber
$c_1 = c_2$	Damping of the absorber
$[H(\omega)]$	Frequency response function
F_a	Preload of the bearing
N_b	Number of balls in the bearing
Ω	Angular velocity in rad/s
$g(\varphi_j)$	Regulating function
θ	Angular contact of the ball bearing
φ_s, φ_e	Entrance and exit angles of the cut

Acknowledgements
We express our sincere gratitude for the support and contributions provided by the National Institute of Technology Rourkela, India, for making this research feasible and laboratory support.

Authors' contributions
Jakeer Hussain played a significant role in the design, methodology, programming in MATLAB, validation, data visualization, and initial draft authoring of the study article. Trivikrama Raju and Yedukondalu contributed to the development of ideas, the collection and organization of data, and the analysis of findings. Murahari contributed to the data collection and manuscript revision. The final version of the manuscript has been reviewed and approved by all authors for publication.

Funding
This research was undertaken without any financial support from public, commercial, or nonprofit funding organizations.

Availability of data and materials
The data substantiating the findings reported in this publication are included inside the article, and no other data sources are required. The datasets will be made available by the corresponding author upon a reasonable request.

Declarations

Competing interests
The authors declare no competing interests.

Received: 9 May 2024 Accepted: 29 June 2024
Published online: 09 July 2024

References

1. Altintas Y, Budak E (1995) Analytical prediction of stability lobes in milling. Annals of the CIRP 44:357–362
2. Chao X, Zhang J, Yu D, Wu Z, Feng J (2015) Dynamics prediction of spindle system using joint models of spindle tool holder and bearings. Proc IMechE Part C: J Mech Eng Sci 229(17):3084–3095
3. Raphael GS, Reginaldo TC (2014) Contribution to improve the accuracy of chatter prediction in machine tools using the stability lobe diagram. J Manf Sci Engg ASME 136:021005–021007

4. Hung JP, Lai YL, Luo TL, Su HC (2013) Analysis of the machining stability of a milling machine considering the effect of machine frame structure and spindle bearings: experimental and finite element approaches. Int J Adv Manf technology 68:2393–2405
5. Albrecht A, Park SS, Altintas Y, Prichstow G (2005) High frequency bandwidth cutting force measurements in milling using capacitance displacement sensors. Int J Mach Tool Manuf 45:993–1008
6. Park SS, Altintas Y (2004) Dynamic compensation of spindle integrated force sensors with Kalman filter. J Dyn Syst Meas Contr 126:443–451
7. Jang JL, Tarng YS (1999) A study of the active vibration control of a cutting tool. J Mater Process Technol 95:78–82
8. Duncan GS, Tummond MF, Schmitz TL (2005) An investigation of the dynamic absorber effect in high-speed machining. Int J Mach Tools Manuf 45:497–507
9. Madoliat R, Hayati S, Ghalebahman AG (2011) Investigation of chatter suppression in slender end mill via a frictional damper. Scientia Iranica B 18(5):1069–1077
10. Parus A, Powałka B, Marchelek K, Domek S, Hoffmann M (2013) Active vibration control in milling flexible workpieces. J Vibration Control 19(7):1103–1120
11. Madoliat R, Hayati S, Ahmad GG (2011) Modeling and analysis of frictional damper effect on chatter suppression in a slender endmill tool. J Adv Mech Design Syst Manuf 5(2):115–128
12. Regib EA, Ni J, Lee SH (2003) Programming spindle speed variation for machine tool chatter suppression. Int J Mach Tools Manuf 43:1229–1240
13. Sulaiman SA, Nurul Amin AKM, Arif MD (2012) Application of permanent magnets for chatter control in end milling of titanium alloy Ti-6Al-4V. Adv Mater Res 576:15–18
14. Monnin J, Kuster F, Wegener K (2014) Optimal control for chatter mitigation in milling-part1: modeling and control design. Control Eng Pract 24:156–166
15. Monnin J, Kuster F, Wegener K (2014) Optimal control for chatter mitigation in milling-part2: experimental validation. Control Eng Pract 24:167–175
16. Graham E, Mehrpouya M, Park SS (2013) Robust prediction of chatter stability in milling based on the analytical chatter stability. J Manuf Process 15:508–517
17. Moradi H, Vossoughi G, Behzad M, Mohammad RM (2015) Vibration absorber design to suppress regenerative chatter in non-linear milling process: application for machining of cantilever plates. Appl Math Model 39:600–620
18. Zhang HT, Wu Y, He D, Zhao H (2015) Model predictive control to mitigate chatters in milling processes with input constraints. Int J Mach Tools Manuf 91:54–61
19. Rafal R, Pawel L, Krzysztof K, Bogdan K, Jerzy W (2015) Chatter identification methods on the basis of time series measured during titanium super alloy milling. Int J Mech Sci 99:196–207
20. Wu H, Wang Y, Li M, Al-Saedi M, Handroos H (2014) Chatter suppression methods of a robot machine for ITER vacuum vessel assembly and maintenance. Fusion Eng Des 89:2357–2362
21. Navid AS, Moradi H, Gholamreza V (2014) Global optimization and design of dynamic absorbers chatter suppression in milling process with tool wear and process damping. Procedia CIRP 21:360–366
22. Vineet P, Ramesh Babua N (2021) Prediction of stability boundaries in milling by considering the variation of dynamic parameters and specific cutting force coefficients. Procedia CIRP 99:183–188
23. Vinh N, Joshua J, Shreyes M (2020) Active vibration suppression in robotic milling using optimal control. Int J Mach Tools Manuf. https://doi.org/10.1016/j.ijmachtools.2020.103541
24. Jérémie M, Fredy K, Konrad W (2014) Optimal control for chatter mitigation in milling—part 1: modeling and control design. Control Eng Pract 24:156–166
25. Rahul K, Sounak KC, Kashfull O (2018) On-line control of machine tool vibration in turning operation using electromagneto rheological damper. J Manuf Process 31:187–198
26. Madoliat R, Hayati S, Ghasemi AG (2011) Investigation of chatter suppression in slender endmill via a frictional damper. Scientia Iranica B 18(5):1069–1077
27. Hans-Christian M, Kim Torben W (2022) Lightweight semi-actively damped high performance milling tool. CIRP Ann Manuf Technol 71:353–356
28. Chen Z, Lu H (2020) Optimal semiactive damping control for a nonlinear energy sink used to stabilize milling. Shock Vib 8837753:1–11. https://doi.org/10.1155/2020/8837753
29. Santiago D et al (2020) Semi-active magnetorheological damper device for chatter mitigation during milling of thin-floor components. Appl Sci 10(15):5313
30. Yang Y, Yu Y (2015) Design and simulation of long slender end mill embedded with passive damper. Procedia Engineering 99:1380–1384
31. Lucia L, Marco S, Rachele B, Andrea G, Stefania B (2021) Surface finish of additively manufactured Ti6Al4V workpieces after ball end milling. Procedia CIRP 102:228–233
32. Gdula M, Mrówka-Nowotnik G (2023) Analysis of tool wear, chip and machined surface morphology in multi-axis milling process of Ni-based superalloy using the torus milling cutter. Wear 520–521:204652